JOURNAL OF CHEMICAL & ENGINEERING DATA

ARTICLE

pubs.acs.org/jced

High-Pressure Adsorption Equilibrium of CO_2, CH_4, and CO on an Impregnated Activated Carbon

Bin Mu and Krista S. Walton*

School of Chemical and Biomolecular Engineering, Georgia Institute of Technology, 311 Ferst Drive NW, Atlanta, Georgia 30332, United States

ABSTRACT: An impregnated activated carbon (I-AC) has been characterized using SEM, EDS, and nitrogen adsorption for micropore structure analysis. A detailed experimental study has been made of the adsorption of pure methane, carbon dioxide, and carbon monoxide at various temperatures [(298 to 318) K] and pressures up to 24 bar. Multitemperature isotherms were modeled using the Toth equation to obtain useful thermodynamic properties including Henry's law constants and isosteric heats of adsorption. Compared with other activated carbon materials, this impregnated carbon has a decreased surface area and more heterogeneous sites on the surface. CO appears to undergo chemisorption in the impregnated carbon, as indicated by a hysteresis loop upon desorption. The effect becomes more pronounced with increasing temperature.

INTRODUCTION

Understanding adsorption in porous materials is a fundamental step in designing adsorption processes including gas separation, purification, and storage.[1−4] Adsorption equilibrium data over a wide range of pressures and temperatures are needed to effectively develop new adsorption processes, understand adsorption mechanisms, and simulate fixed-bed systems. The need for single-component adsorption data is still most important in this regard. Single-component adsorption equilibrium experiments are used to characterize different adsorbent surfaces and investigate the nature of their interactions with the adsorbate molecules. Thanks to high-quality adsorption equilibrium data, various adsorption models can be developed more accurately to elucidate the adsorption mechanism and simplify the design process. Furthermore, thermodynamic properties, which can be derived from isotherm data, including Henry's law constants, isosteric heats, heat capacities, and the entropy change on adsorption, are required for simulating cyclic nonisothermal adsorption processes such as temperature and pressure swing adsorption. Thus, it is difficult or even impossible without the knowledge of the adsorption equilibrium to simulate and design an adsorption process.[5]

Among the porous materials used commercially, activated carbon is one of the most complex and also one of the most widely studied. However, single-component adsorption isotherms measured over ranges of pressure and temperature on impregnated activated carbons (I-AC) are relatively scarce in the literature. The I-AC studied here is BPL activated carbon (manufactured by Calgon Carbon Corporation) impregnated primarily with copper and zinc. Water isotherms have been reported for a similar material,[6] but no studies have been published on the adsorption of carbon dioxide, carbon monoxide, and methane. This paper presents experimental adsorption and desorption isotherms of CO_2, CH_4, and CO on I-AC over the temperature range (25 to 45) °C and a wide range of pressures from (0 to 24) bar. Furthermore, the adsorption isotherms on the I-AC are compared with the isotherms from BPL and other activated carbons by fitting the data to the Toth equation.

MATERIALS, METHODS, AND CHARACTERIZATION

BPL carbon (Calgon Carbon Corporation) is produced from bituminous coal and is highly activated to give a surface area and pore volume of approximately 1250 $m^2 \cdot g^{-1}$ and 0.56 $cm^3 \cdot g^{-1}$, respectively.[7] The carbon has substantial meso- and macroporosity to provide for rapid internal mass transfer and to accommodate the application of the reactive impregnates. Scanning electron microscopy (SEM) images (Figure 1) were conducted on a Hitachi SEM S-3500N equipped with a model S-6542 absorbed electron detector, and the compositional analysis was obtained by energy dispersive spectroscopy (EDS, Oxford-INCA). SEM results present apparent irregularity of the I-AC in shape, and particle size is around millimeters to micrometers. Such roughness of the surface is favorable to increase the interspace among particles and to increase adsorption amount on the adsorbent's surface. The compositional analysis given in Figure 2 shows that the primary impregnate loadings are 4.4 wt % copper and 4.1 wt % zinc.

A nitrogen adsorption isotherm (Figure 3) of the I-AC at 77 K was measured with Autosorb-1 from the Quantachrome Corporation. The isotherm presents a major type-I Langmuir isotherm together with a minor type-II isotherm near the saturated vapor pressure, indicating monolayer coverage may be complete. In addition, a slight hysteresis loop appears at higher pressure, which was closed at about $P/P_0 = 0.4$. Specific surface areas calculated using the BET and Langmuir models are 922 $m^2 \cdot g^{-1}$ and 1238 $m^2 \cdot g^{-1}$, respectively. The BET constant and Langmuir constant are 799.4 and 38.5, respectively, in which

Received: July 22, 2010
Accepted: January 3, 2011
Published: February 04, 2011

dx.doi.org/10.1021/je1007668 | *J. Chem. Eng. Data* 2011, 56, 390–397

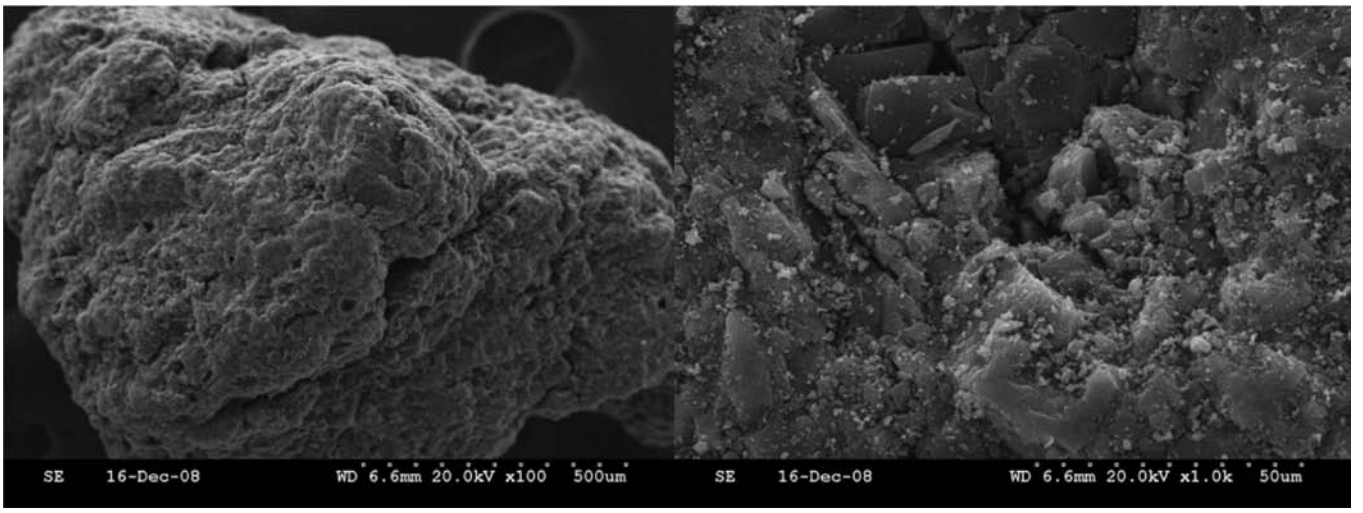

Figure 1. SEM images of the I-AC.

Element	Weight %	Atomic %
C K	78.01	87.09
O K	12.29	10.29
Al K	0.29	0.14
Si K	0.38	0.18
S K	0.45	0.19
Cu K	4.43	0.94
Zn K	4.15	0.85
Totals	100.00	

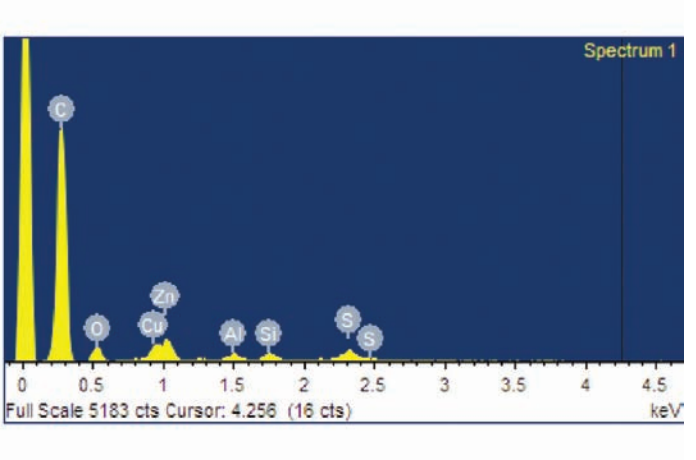

Figure 2. Compositional analysis of the I-AC using energy dispersive spectroscopy (EDS, Oxford-INCA).

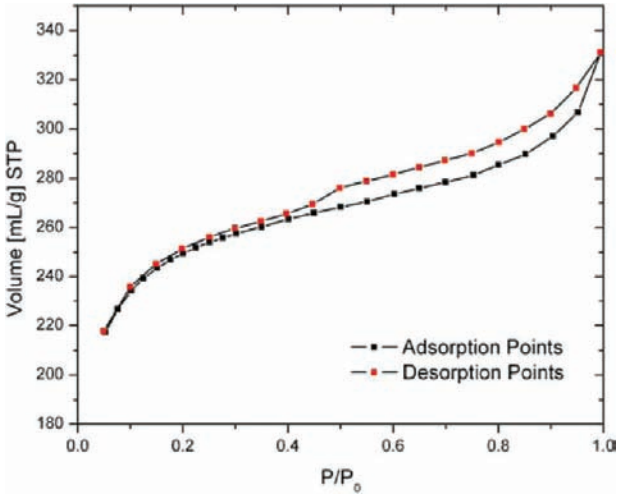

Figure 3. Nitrogen isotherm at 77 K.

the linear BET region for the I-AC occurs at relative pressures lower than 0.12, while the linear Langmuir region for the I-AC occurs at relative pressures lower than 0.70. The total pore volume is 0.51 mL·g^{-1} at $P/P_0 = 0.99513$, while the average pore diameter is 2.22 nm. A t-plot was fitted with the de Boer equation (Figure 4). The pore size distribution was calculated using the Dubinin−Astakhov (DA) method, as shown in Figure 5, and the micropore structure analysis results are listed in Table 1.

A gravimetric adsorption apparatus (the GHP-100 gravimetric high-pressure analyzer with C. I. microbalance from the VTI Corporation) was employed to measure the single-component adsorption isotherms. All adsorbate gases were purchased from the Linweld Company including carbon dioxide (LW617, bone dry 99.8 %), methane (LW913, ultrahigh purity 99.99 %), carbon monoxide (LW609, CP 99.5 %), helium (LW800, UHP/ZERO), and nitrogen (LW411, UHP/ZERO). Before the adsorption measurement, the I-AC was activated by heating at 120 °C in a vacuum for 24 h to remove moisture and other adsorbed gases. A 150 mg sample was placed in the sample cartridge of the GHP-100 gravimetric high-pressure analyzer to undergo continued outgassing at 110 °C in a vacuum for 12 h. The sample weight was recorded every 2 min or per 0.01 % by mass. After outgassing, the system temperature was adjusted to the adsorption temperature of interest, and the sample cell was kept under a vacuum for 30 min before starting the first adsorption point. All adsorption equilibrium data were collected after maintaining a given stable

dx.doi.org/10.1021/je1007668 |J. Chem. Eng. Data 2011, 56, 390–397

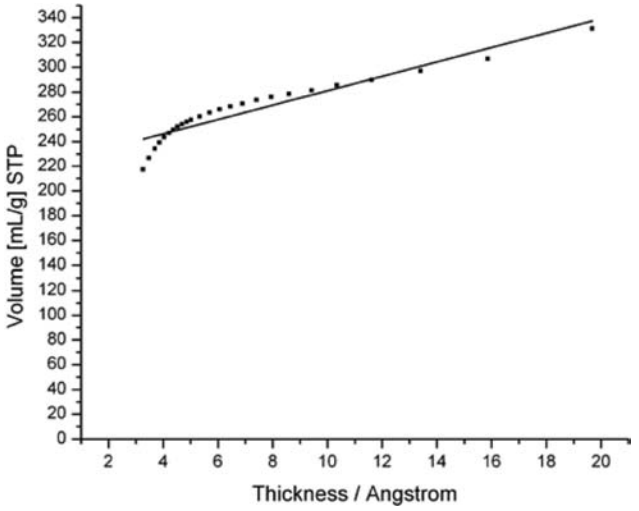

Figure 4. t-plot of the I-AC.

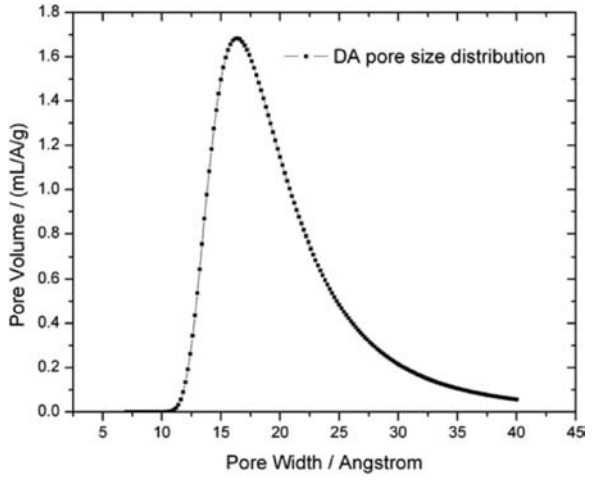

Figure 5. DA pore size distribution plot.

Table 1. Micropore Structure Analysis of I-AC

N_2 isotherm	total pore volume/mL·g^{-1}	0.51
	average pore diameter/nm	2.22
	hysteresis loop rang (P/P_0)	0.4−1.0
BET method	surface area/m^2·g^{-1}	922
	BET constant	799.4
	linear range	0.05−0.12
Langmuir method	surface area/m^2·g^{-1}	1238
	langmuir constant	38.5
	linear range	0.05−0.70
t-plot (de Boer equation)	slope	5.801
	y-intercept	223.036
	external surface area/m^2·g^{-1}	89.7
	micropore volume/mL·g^{-1}	0.345
	micropore area/m^2·g^{-1}	831.9
D-A method	characteristic energy/kJ·mol^{-1}	6.00
	n	1.90
	pore diameter/nm	1.64

pressure for 30 min. After finishing the adsorption and desorption runs at the given temperature, the I-AC was regenerated by heating at 110 °C in a vacuum for 12 h until a constant sample weight was achieved. The sample was then reused in subsequent adsorption experiments.

Table 2. Experimental Adsorption Equilibrium Loadings (N) of CH_4 on I-AC Including Desorption Points

298 K		308 K		318 K	
P/bar	N/mmol·g^{-1}	P/bar	N/mmol·g^{-1}	P/bar	N/mmol·g^{-1}
0.099	0.124	0.102	0.039	0.101	0.026
0.199	0.177	0.222	0.081	0.201	0.076
0.297	0.224	0.305	0.129	0.299	0.124
0.394	0.270	0.395	0.169	0.394	0.170
0.528	0.335	0.551	0.242	0.526	0.230
0.649	0.389	0.668	0.294	0.651	0.282
0.780	0.446	0.780	0.341	0.784	0.335
0.972	0.527	0.975	0.421	0.972	0.407
1.937	0.878	1.939	0.753	1.942	0.717
3.102	1.195	3.104	1.060	3.103	1.016
5.162	1.617	5.167	1.482	5.171	1.419
6.481	1.832	6.490	1.699	6.487	1.625
9.127	2.179	9.130	2.048	9.130	1.973
11.642	2.440	11.644	2.308	11.647	2.225
12.996	2.562	13.002	2.421	13.001	2.348
17.060	2.865	17.062	2.737	17.065	2.659
20.940	3.094	20.942	2.986	20.940	2.877
24.237	3.258	24.237	3.157	24.238	3.068
20.949	3.096	20.955	2.986	20.918	2.898
17.166	2.873	17.183	2.754	17.153	2.670
13.738	2.625	13.725	2.501	13.745	2.415
11.073	2.388	11.074	2.265	11.063	2.201
7.562	1.987	7.549	1.865	7.543	1.787
4.117	1.420	4.122	1.306	4.116	1.251
2.058	0.907	2.060	0.811	2.057	0.766
1.366	0.673	1.372	0.591	1.375	0.561
1.022	0.534	1.023	0.463	1.022	0.439
0.820	0.442	0.819	0.380	0.819	0.361
0.682	0.375	0.681	0.321	0.682	0.306
0.545	0.303	0.547	0.258	0.537	0.244
0.393	0.214	0.410	0.188	0.409	0.185
		0.272	0.112	0.265	0.113
		0.103	0.002		

RESULTS AND DISCUSSION

Adsorption Isotherms. The data for adsorption and desorption of methane, carbon dioxide, and carbon monoxide on the I-AC were obtained for temperatures ranging from (298 to 318) K and pressures up to 24 bar. The maximum adsorption capacities of CH_4 on the I-AC at 298 K, 308 K, and 318 K are (3.26, 3.16, and 3.07) mmol·g^{-1}, respectively, at 24.2 bar (Table 2). The maximum capacities of CO_2 at 298 K, 308 K, and 318 K are (6.15, 5.83, and 5.59) mmol·g^{-1}, respectively, at 24.2 bar (Table 3), and the capacities of CO at these temperatures are (2.01, 2.06, and 2.21) mmol·g^{-1}, respectively, at 17.1 bar (Table 4). For CH_4 and CO_2, the adsorption isotherms are reversible, and there is no hysteresis in the range of examined temperature and pressure (Figures 6 and 7). However, CO

dx.doi.org/10.1021/je1007668 |J. Chem. Eng. Data 2011, 56, 390–397

Table 3. Experimental Adsorption Equilibrium Loadings (N) of CO_2 on I-AC Including Desorption Points

298 K		308 K		318 K	
P/bar	N/mmol·g^{-1}	P/bar	N/mmol·g^{-1}	P/bar	N/mmol·g^{-1}
0.100	0.308	0.098	0.250	0.098	0.210
0.202	0.496	0.204	0.421	0.200	0.355
0.304	0.655	0.306	0.559	0.293	0.468
0.389	0.770	0.409	0.680	0.390	0.574
0.524	0.936	0.534	0.814	0.527	0.707
0.648	1.073	0.648	0.925	0.650	0.820
0.775	1.201	0.813	1.073	0.776	0.927
0.969	1.381	0.965	1.200	1.005	1.098
1.938	2.074	1.937	1.834	1.938	1.683
3.131	2.701	3.128	2.425	3.097	2.213
5.157	3.467	5.158	3.151	5.163	2.915
6.477	3.852	6.479	3.523	6.482	3.269
9.124	4.448	9.124	4.102	9.124	3.831
11.633	4.879	11.636	4.526	11.630	4.275
12.989	5.082	12.991	4.722	12.987	4.469
17.063	5.558	17.060	5.203	17.052	4.969
20.933	5.911	20.933	5.570	20.930	5.338
24.225	6.149	24.233	5.828	24.227	5.587
20.966	5.923	20.957	5.577	20.966	5.348
17.175	5.558	17.178	5.248	17.175	4.991
13.791	5.159	13.729	4.855	13.791	4.627
11.079	4.766	11.077	4.491	11.079	4.261
7.575	4.106	7.562	3.850	7.575	3.622
4.129	3.135	4.124	2.911	4.129	2.725
2.065	2.192	2.065	2.022	2.065	1.887
1.376	1.736	1.376	1.612	1.376	1.497
1.027	1.451	1.025	1.356	1.027	1.269
0.822	1.258	0.821	1.191	0.822	1.107
0.684	1.115	0.683	1.069	0.684	0.992
0.548	0.959	0.547	0.940	0.548	0.871
0.391	0.756	0.410	0.794	0.391	0.718
0.260	0.560			0.260	0.575
0.100	0.264			0.100	0.360

Table 4. Experimental Adsorption Equilibrium Loadings (N) of CO on I-AC Including Desorption Points

298 K		308 K		318 K	
P/bar	N/mmol·g^{-1}	P/bar	N/mmol·g^{-1}	P/bar	N/mmol·g^{-1}
0.101	0.046	0.100	0.037	0.101	0.087
0.194	0.078	0.196	0.061	0.196	0.120
0.292	0.112	0.294	0.086	0.293	0.150
0.390	0.144	0.390	0.111	0.390	0.178
0.523	0.186	0.528	0.145	0.525	0.213
0.650	0.223	0.649	0.175	0.667	0.248
0.776	0.257	0.776	0.205	0.778	0.276
0.972	0.306	0.970	0.249	0.970	0.320
1.163	0.352	1.166	0.292	1.165	0.363
1.681	0.464	1.681	0.396	1.680	0.460
1.940	0.516	1.940	0.445	1.961	0.514
3.102	0.719	3.101	0.640	3.122	0.706
3.896	0.840	3.895	0.765	3.876	0.825
5.153	1.009	5.154	0.947	5.154	1.027
6.480	1.166	6.477	1.120	6.476	1.208
9.122	1.429	9.124	1.398	9.121	1.496
11.639	1.640	11.642	1.630	11.638	1.749
12.996	1.743	12.996	1.743	12.995	1.877
16.161	1.954	16.159	1.977	16.160	2.126
17.066	2.011	17.065	2.057	17.067	2.209
13.743	1.815	13.730	1.873	13.738	2.040
11.050	1.629	11.076	1.704	11.083	1.879
7.554	1.330	7.558	1.420	7.556	1.611
4.124	0.939	4.122	1.042	4.123	1.259
2.061	0.617	2.060	0.738	2.063	0.974
1.374	0.482	1.374	0.614	1.374	0.861
1.025	0.405	1.026	0.544	1.026	0.797
0.820	0.356	0.819	0.501	0.820	0.757
0.545	0.286	0.681	0.470	0.682	0.729
0.274	0.208	0.547	0.439	0.530	0.697
0.098	0.151	0.398	0.404	0.410	0.670
		0.272	0.371	0.273	0.637
		0.098	0.323	0.101	0.591

appears to undergo chemisorption and displays a hysteresis loop upon desorption that becomes more pronounced with increasing temperature (Figure 8 and 9).

Because of the simplicity of the Toth equation in form and its correct thermodynamic consistency at low and high pressures, it has been recommended for fitting the adsorption isotherms of hydrocarbons on activated carbon.[8] The Toth equation has also been used successfully to fit CO_2 and CH_4 adsorption data in a variety of activated carbons (Table 5).[9−14] The Toth equation is given by

$$N = \frac{N_s bP}{[1 + (bP)^m]^{1/m}} \quad (1)$$

where N_s is the monolayer capacity; b is related to the adsorption affinity at low pressure; and m characterizes the system heterogeneity. The deviation of m from unity indicates the heterogeneity of the system. When $m = 1$, the Toth equation reduces to the Langmuir equation. Using the Toth equation parameters listed in Table 5, CH_4 and CO_2 isotherms of various activated carbons at 298 K are graphically presented in Figure 10 and Figure 11 for direct comparison with I-AC. The BET surface area and total pore volume of the various activated carbons are listed in Table 6 for further comparison.

Among the examined activated carbons, Maxsorb has the highest surface area and the largest total pore volume. Thus, it is not surprising for it to present the highest adsorption capacities for CH_4. As shown in Table 5, the parameter m from Calgon-AC is the closest to unity at room temperature, which indicates that Calgon-AC is more homogeneous than other activated carbons. Activated carbon obtained from coconut shells (Coconut-AC) demonstrates unexpectedly low CH_4 capacity considering its high surface area. However, at low pressure, it presents higher adsorption loadings compared to I-AC and BPL, which is consistent with the higher adsorption affinity parameter b of Coconut-AC. With an increase in pressure, its capacity does not increase significantly and is much less than that of BPL and I-AC at 24 bar due to the low monolayer capacity. These experimental results also confirm

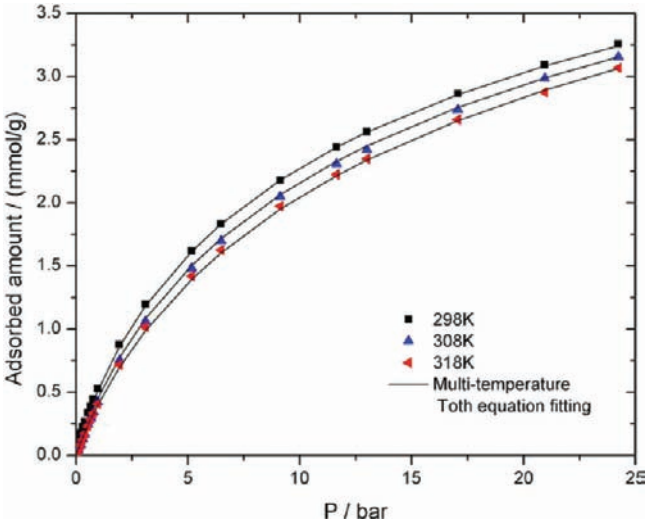

Figure 6. CH_4 isotherms on the I-AC at different temperatures.

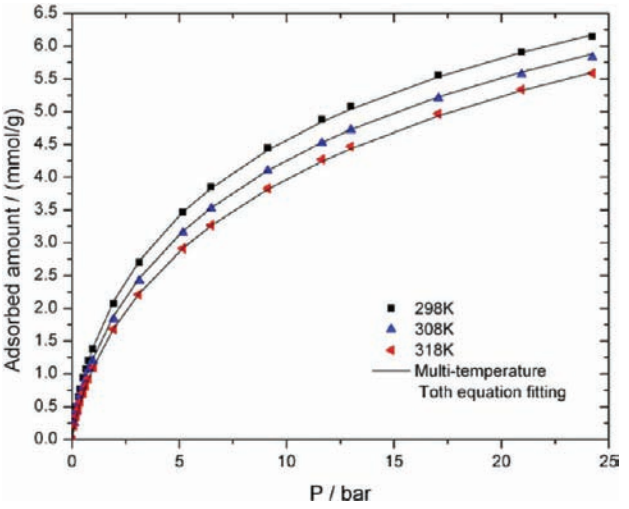

Figure 7. CO_2 isotherms on the I-AC at different temperatures.

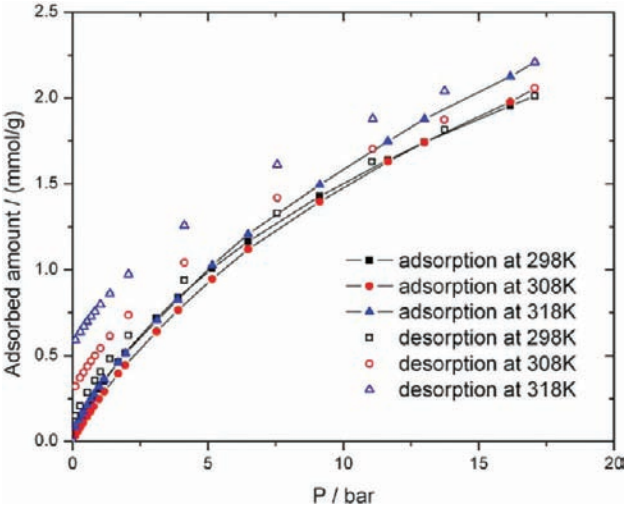

Figure 8. CO isotherms on I-AC at different temperatures.

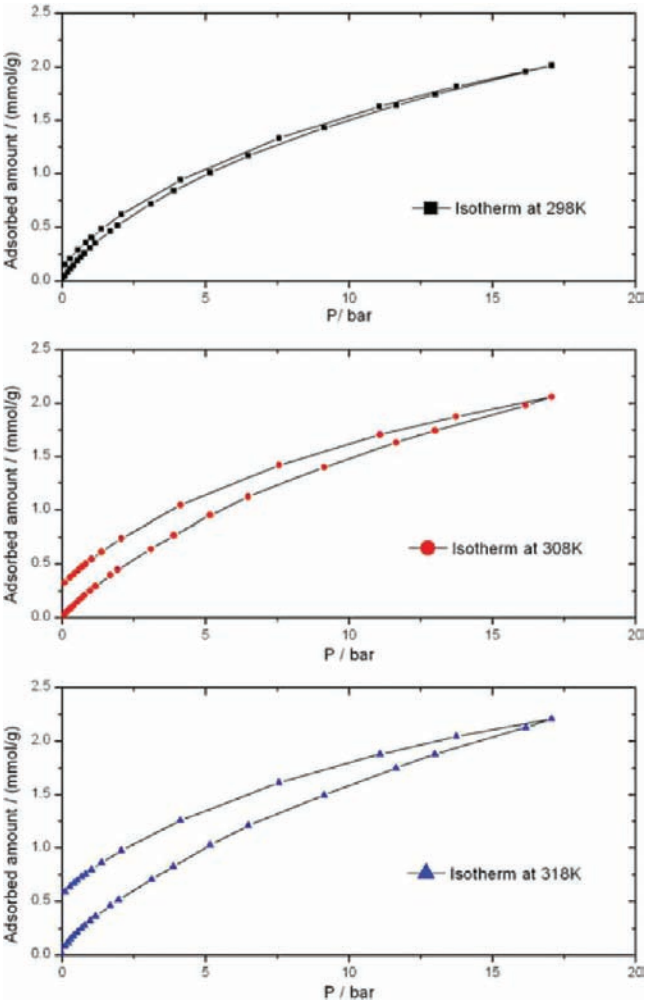

Figure 9. Development of CO hysteresis loop with increasing temperature.

the conclusion of Bhatia and Myers.[15] They studied the effect of heterogeneity on adsorptive storage of H_2 and CH_4 on activated carbon from a thermodynamic viewpoint and demonstrated that heterogeneity is less helpful and even detrimental for CH_4 storage on activated carbon. The impregnated activated carbon has less surface area and total pore volume than BPL, which is responsible for the decreased adsorption capacities of CH_4. For CO_2 adsorption equilibrium, the isotherms followed the order of increasing capacity with increasing surface area (Figure 11).

Henry's Law Constants and Heat of Adsorption. Henry's law constants k_H were calculated from the product of the Toth equation parameters $N_s \cdot b$, which indicates the affinity between the sorbate and sorbent surface at low coverage. The Henry's law constants are listed in Table 7,[9−14,16] and the values from I-AC and BPL are graphically presented as a function of temperature in Figure 12. From Table 7 and Figure 12, we can observe that Henry's law constants of CH_4 for I-AC are slightly smaller than the corresponding values for BPL within the examined temperature range, and k_H values for both CH_4 and CO_2 decrease with an increase of temperature.

The isosteric heat of adsorption on the I-AC is calculated by the Clausius−Clapeyron equation combined with the

Table 5. Toth Equation Parameters for Different Activated Carbons

		CH_4			CO_2			CO		
adsorbents	T/K	N_s/mmol·g^{-1}	b/bar^{-1}	m	N_s/mmol·g^{-1}	b/bar^{-1}	m	N_s/mmol·g^{-1}	b/bar^{-1}	m
I-AC	298	7.509	0.128	0.527	13.79	0.296	0.439	10.36	0.053	0.437
	308	5.624	0.094	0.744	14.14	0.232	0.437	9.391	0.035	0.553
	318	5.741	0.091	0.714	14.65	0.186	0.436	10.20	0.044	0.496
BPL[9]	273	6.813	0.300	0.647	13.70	0.540	0.561			
	298	6.809	0.180	0.616	12.00	0.384	0.533			
	323	7.686	0.095	0.578	9.438	0.134	0.77			
Norit R1 Extra[9]	298	10.80	0.184	0.525	16.8	0.223	0.583			
Maxsorb[9]	298	20.35	0.064	0.768	41.88	0.058	0.827			
A10[9]	298	7.573	0.220	0.658	11.07	0.330	0.744			
AC-A[9]	298	7.524	0.241	0.717	10.43	0.384	0.817			
Coconut-AC[10]	298	3.109	0.336	1.382						
BDH-AC[12]	303	2.367	0.361	0.878						
F30/470-AC[13]	303	1.767	0.14	0.761						
Calgon-AC[11]	293	5.812	0.173	0.998						
	303	5.272	0.147	1.085						
RP-15[14]	293	8.688	0.217	0.776						
	303	8.904	0.232	0.773						
	313	9.563	0.153	0.665						
RP-20[14]	293	11.67	0.173	0.694						
	303	11.514	0.136	0.693						
	313	12.484	0.101	0.650						

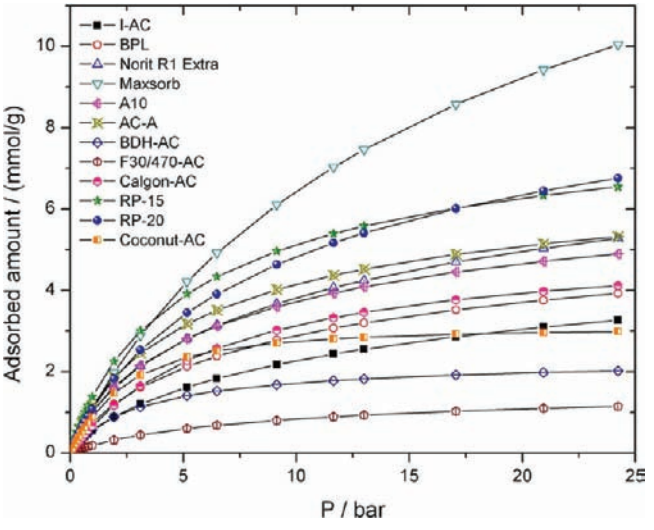

Figure 10. Comparison of CH_4 isotherms at 298 K on varied activated carbons calculated using the Toth equation (the data of BDH-AC, F30/470-AC, Calgon-AC, RP-15, and RP-20 are at 303 K, while others are at 298 K).

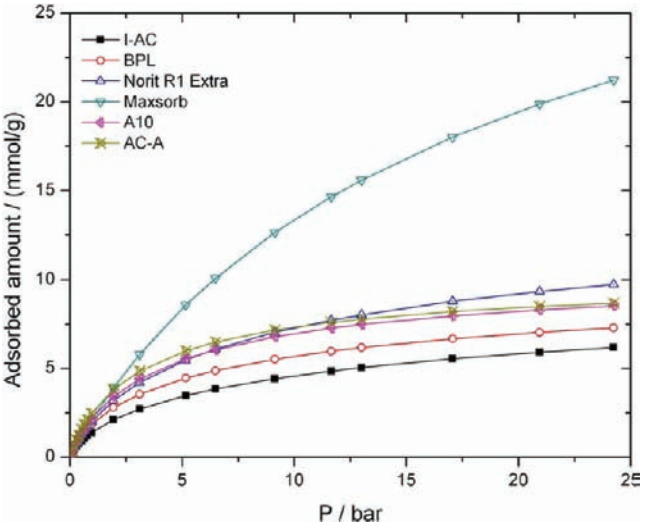

Figure 11. Comparison of CO_2 isotherms at 298 K on various activated carbons calculated using the Toth equation.

multitemperature Toth equation, given by

$$N = \frac{N_s bP}{[1+(bP)^m]^{1/m}} \quad (2)$$

$$b = b_0 \exp\left[\frac{Q}{RT_0}\left(\frac{T_0}{T}-1\right)\right] \quad (3)$$

$$m = m_0 + a\left(1-\frac{T_0}{T}\right) \quad (4)$$

$$N_s = N_{s,0} \exp\left[c\left(1-\frac{T}{T_0}\right)\right] \quad (5)$$

where T_0 is the reference temperature, 318 K; b_0 is the adsorption affinity at the reference temperature; Q is the heat of adsorption at zero coverage; $N_{s,0}$ is the monolayer capacity at the reference temperature; m_0 indicates heterogeneity of the system at the reference temperature; and a and c are fitting parameters that do not have a sound theoretical basis.[8] The comparison of experimental adsorption data and the multitemperature Toth equation fitting is graphically displayed in Figures 6 and 7, and the

dx.doi.org/10.1021/je1007668 |J. Chem. Eng. Data 2011, 56, 390–397

Table 6. Surface Area and Total Pore Volume of Activated Carbons

adsorbent	I-AC	BPL[7]	Norit R1 Extra[9]	Maxsorb[9]	A10[9]	AC-A[9]
BET ($m^2 \cdot g^{-1}$)	922	1250	1450	3250	1200	1207
V ($mL \cdot g^{-1}$)	0.51	0.56	0.47	1.79	0.53	0.54
adsorbent	BDH-AC[12]	F30/470-AC[13]	Coconut-AC[10]	RP-15[14]	RP-20[14]	Calgon_AC[11]
BET ($m^2 \cdot g^{-1}$)	1220	994	2100	1493	1853	1200
V ($mL \cdot g^{-1}$)	0.534	0.497	–	0.658	0.765	0.72

Table 7. Henry's Law Constants

		CH_4	CO_2
adsorbents	T/K	k_H/mol·kg^{-1}·bar^{-1}	k_H/mol·kg^{-1}·bar^{-1}
I-AC	298	0.961	4.082
	308	0.529	3.280
	318	0.522	2.725
BPL[9]	273	2.044	7.398
	298	1.226	4.608
	323	0.730	1.265
Norit R1 Extra[9]	298	1.987	3.746
Norit R1 Extra[16]	298	1.724	4.737
Maxsorb[9]	298	1.302	2.429
A10[9]	298	1.666	3.653
AC-A[9]	298	1.813	4.005
Coconut-AC[10]	298	1.045	
BDH-AC[12]	303	0.854	
F30/470-AC[13]	303	0.247	
Calgon-AC[11]	293	1.005	
	303	0.775	
RP-15[14]	293	1.885	
	303	2.066	
	313	1.463	
RP-20[14]	293	2.019	
	303	1.566	
	313	1.261	

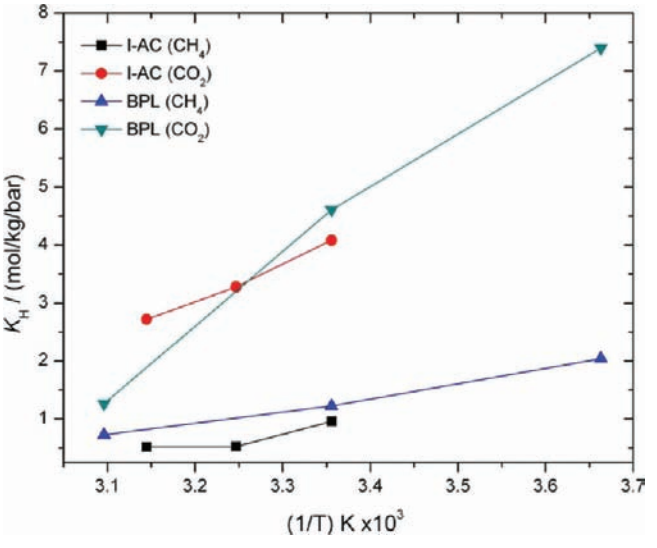

Figure 12. Henry's law constants at different temperatures.

Table 8. Multitemperature Toth Equation Parameters for Describing CH_4 and CO_2 Isotherms on the I-AC

	CH_4	CO_2
$N_{s,0}$	6.35457	14.74364
b_0	0.08403	0.18622
$Q/(RT_0)$	5.65244	6.8373
m_0	0.66427	0.43307
a	0.47176	−0.10344
c	−0.4773	−1.13972
T_0	318	318
Chi^2/DoF	0.00056	0.00062
R^2	0.99958	0.99986
ARE, %	9.19	1.92

Table 9. Comparison of Heats of Adsorption for Various Activated Carbons at Zero Coverage

	heat of adsorption/kJ·mol^{-1}	
adsorbents	CH_4	CO_2
I-AC	14.9	18.2
BPL[9]	16.1	25.7
Norit R1 Extra[9]	20.6	22
Maxsorb[9]	16.3	16.2
A10[9]	16.2	21.6
AC-A[9]	18.3	17.8
Norit RB1[18]	19.5	23.5
Coconut-AC[10]	18.6	
BDH-AC[12]	25.4	
BAX-1100[17]	24.5	
Calgon-AC[11]	27.5	
RP-15[14]	11.4	
RP-20[14]	18.3	

parameters are given in Table 8. The multitemperature Toth equation provides a very successful fit of our experimental data. Thus, the isosteric heat of adsorption for CH_4 and CO_2 can be calculated from the fitting parameters. As presented in Figure 13, the isosteric heat of adsorption for CO_2 increases substantially with an increase in the loading, which demonstrates that adsorbate interactions between CO_2 molecules are becoming more significant. As for CH_4, the negligible intermolecular interaction between CH_4 molecules causes a decrease in the isosteric heat of adsorption as a result of the disappearance of favorable adsorption sites. The heats of adsorption near zero coverage for various activated carbons are listed in Table 9.[9−14,16−18] Among all examined activated carbons, Calgon-AC has the highest heat of

dx.doi.org/10.1021/je1007668 |J. Chem. Eng. Data 2011, 56, 390–397

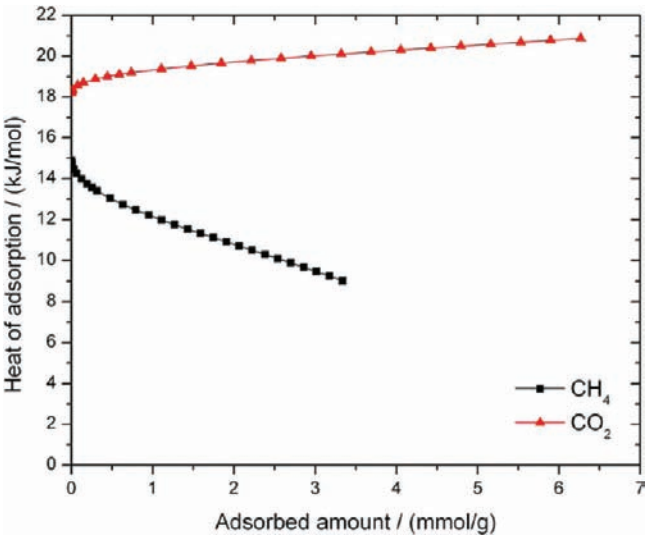

Figure 13. Isosteric heat of adsorption of CH_4 and CO_2 on the I-AC.

adsorption for CH_4, while BPL AC has the highest heat of adsorption for CO_2. The heats of adsorption for CO_2 are consistent with Henry's constants, but no clear correlation is observed for methane. Compared with BPL AC, the heats of adsorption for CH_4 and CO_2 on the I-AC decrease 7.5 % and 29.2 %, respectively, implying a negative effect of the impregnated form to CH_4 and CO_2 adsorption.

CONCLUSIONS

A detailed micropore structure analysis and surface characterization of an impregnated activated carbon (I-AC) were presented with the help of a nitrogen adsorption isotherm and SEM technique. Adsorption equilibrium data of methane, carbon dioxide, and carbon monoxide on the I-AC were obtained at 298 K, 308 K, and 318 K and pressures up to 24 bar. CH_4 and CO_2 presented reversible adsorption isotherms, while CO displayed strong chemisorption that became more pronounced at higher temperatures. The adsorption data of CH_4 and CO_2 were correlated by the Toth equation and further by the multitemperature Toth equation. The fitting details demonstrated that the multitemperature Toth equation is a powerful tool to mathematically represent the CH_4 and CO_2 isotherms on the I-AC. In addition, the experimental data confirmed the conclusion of Bhatia and Myers that the impregnation method is harmful to the adsorption capacity of CH_4. Finally, Henry's law constants and heats of adsorption near zero coverage of the I-AC were calculated and compared with the values from various activated carbons.

AUTHOR INFORMATION

Corresponding Author

*E-mail: krista.walton@chbe.gatech.edu.

Funding Sources

This material is based upon work supported by the Army Research Office under contract W911NF-10-1-0076.

REFERENCES

(1) Ma, S. Q. Gas adsorption applications of porous metal-organic frameworks. *Pure Appl. Chem.* **2009**, *81*, 2235–2251.

(2) Li, J. R.; Kuppler, R. J.; Zhou, H. C. Selective gas adsorption and separation in metal-organic frameworks. *Chem. Soc. Rev.* **2009**, *38*, 1477–1504.

(3) Mu, B.; Schoenecker, P. M.; Walton, K. S. Gas Adsorption Study on Mesoporous Metal-Organic Framework UMCM-1. *J. Phys. Chem. C* **2010**, *114*, 6464–6471.

(4) Mu, B.; Li, F.; Walton, K. S. A novel metal-organic coordination polymer for selective adsorption of CO2 over CH4. *Chem. Commun.* **2009**, 2493–2495.

(5) Yang, R. T. *Gas separation by adsorption processes*; Butterworths: Boston, 1987; p. 352.

(6) Sullivan, P. D.; Stone, B. R.; Hashisho, Z.; Rood, M. J. Water adsorption with hysteresis effect onto microporous activated carbon fabrics. *Adsorption* **2007**, *13*, 173–189.

(7) Furukawa, H.; Yaghi, O. M. Storage of Hydrogen, Methane, and Carbon Dioxide in Highly Porous Covalent Organic Frameworks for Clean Energy Applications. *J. Am. Chem. Soc* **2009**, *131*, 8875–8883.

(8) Duong, D. D. *Adsorption analysis: equilibria and kinetics*; Imperial College Press: London, 1998; p. xxi.

(9) Himeno, S.; Komatsu, T.; Fujita, S. High-pressure adsorption equilibria of methane and carbon dioxide on several activated carbons. *J. Chem. Eng. Data* **2005**, *50*, 369–376.

(10) Walton, K. S.; Cavalcante, C. L.; Levan, M. D. Adsorption of light alkanes on coconut nanoporous activated carbon. *Braz. J. Chem. Eng.* **2006**, *23*, 555–561.

(11) Choi, B. U.; Choi, D. K.; Lee, Y. W.; Lee, B. K.; Kim, S. H. Adsorption equilibria of methane, ethane, ethylene, nitrogen, and hydrogen onto activated carbon. *J. Chem. Eng. Data* **2003**, *48*, 603–607.

(12) Al-Muhtaseb, S. A.; Abu Al-Rub, F. A.; Al Zarooni, M. Adsorption equilibria of nitrogen, methane, and ethane on BDH-activated carbon. *J. Chem. Eng. Data* **2007**, *52*, 60–65.

(13) Frere, M. G.; De Weireld, G. F. High-pressure and high-temperature excess adsorption isotherms of N-2, CH4, and C3H8 on activated carbon. *J. Chem. Eng. Data* **2002**, *47*, 823–829.

(14) Lee, J. W.; Balathanigaimani, M. S.; Kang, H. C.; Shim, W. G.; Kim, C.; Moon, H. Methane storage on phenol-based activated carbons at (293.15, 303.15, and 313.15) K. *J. Chem. Eng. Data* **2007**, *52*, 66–70.

(15) Bhatia, S. K.; Myers, A. L. Optimum conditions for adsorptive storage. *Langmuir* **2006**, *22*, 1688–1700.

(16) Dreisbach, F.; Staudt, R.; Keller, J. U. High pressure adsorption data of methane, nitrogen, carbon dioxide and their binary and ternary mixtures on activated carbon. *Adsorpt.-J. Int. Adsorpt. Soc.* **1999**, *5*, 215–227.

(17) Holland, C. E.; Al-Muhtaseb, S. A.; Ritter, J. A. Adsorption of C-1-C-7 normal alkanes on BAX activated carbon. 1. Potential theory correlation and adsorbent characterization. *Ind. Eng. Chem. Res.* **2001**, *40*, 338–346.

(18) Van der Vaart, R.; Huiskes, C.; Bosch, H.; Reith, T. Single and mixed gas adsorption equilibria of carbon dioxide/methane on activated carbon. *Adsorpt.-J. Int. Adsorpt. Soc.* **2000**, *6*, 311–323.